Fisheries Research 121-122 (2012) 144–152

Contents lists available at SciVerse ScienceDirect

Fisheries Research

journal homepage: www.elsevier.com/locate/fishres

Testing early life connectivity supplying a marine fishery around the Falkland Islands

Julian R. Ashford[a,*], Bettina A. Fach[b], Alexander I. Arkhipkin[c], Cynthia M. Jones[a]

[a] Center for Quantitative Fisheries Ecology, Old Dominion University, 800 West 46th St., Norfolk, VA 23529, USA
[b] Institute of Marine Sciences, Middle East Technical University, PO Box 28, 33731 Erdemli, Turkey
[c] Fisheries Department, Falkland Islands Government, Stanley, Falkland Islands

ARTICLE INFO

Article history:
Received 14 September 2011
Received in revised form 21 January 2012
Accepted 24 January 2012

Keywords:
Immigration
Population structure
Patagonian toothfish
Patagonian Shelf
Member-vagrant hypothesis
Antarctic Circumpolar Current
Subantarctic Front

ABSTRACT

We used a wind-driven global circulation model to build spatially explicit predictions from rival hypotheses concerning advective supply of Patagonian toothfish (*Dissostichus eleginoides*) to a trawl fishery around the Falkland Islands, and tested the predictions using chemistry recorded in the otoliths of fish caught in the fishery. Model simulations indicated transport pathways from spawning aggregations off southern Chile to both the north and south of the fishing area. In contrast, simulated particles released from spawning aggregations around Burdwood Bank were transported to the south of the fishing area but not to the north, becoming fully entrained in the Subantarctic Front instead. Spatial heterogeneity in the chemistry laid down in the otolith nuclei during early life discounted the hypothesis of a single population with a spawning area on Burdwood Bank, and indicated that fish assemblages are structured by large-scale transport from both southern Chile and Burdwood Bank. By linking fish explicitly to their physical environment, the two techniques can help distinguish the life cycle trajectories necessary for populations to persist, and elucidate the interactions between hydrography and life history that structure the fish assemblages on which marine fisheries depend.

1. Introduction

1.1. Competing life history hypotheses

Many marine fisheries target fish stocks that are structured by their physical environment; as a result, the spatial relationships between physical and biological processes are potentially key to understanding their distribution and abundance. In populations that are geographically contained by barriers like oceanic fronts or deep water (e.g. Kingsford, 1993; Loeb et al., 1993), the dynamics are defined by births and deaths of inter-breeding fish isolated within discrete domains that can be managed independently, and the life-cycle is closed through local retention and self-recruitment (e.g. Almany et al., 2007). However, dispersal and movement can connect geographically distant areas, giving coherence to life history cycles in which life stages take advantage of different habitats (e.g. Harden Jones, 1968; Cushing, 1981; Thorrold et al., 2001). Moreover, immigration from outside sources can subsidize populations in which low self-recruitment relative to mortality otherwise leads to extinction (Pulliam, 1988). Since dispersal often occurs during early life before active movement is well developed, the large-scale circulation can strongly influence the direction and extent of connections between habitats and populations, and hence the spatial composition of the fish assemblages which fisheries harvest.

Around the Falkland Islands off south-eastern South America, a longline fishery harvests adult Patagonian toothfish (*Dissostichus eleginoides*) along the continental slope (e.g. Laptikhovsky et al., 2006). Greater numbers, however, are caught as juveniles in a trawl fishery in the Falkland Islands Interim Conservation and Management Zone (FICZ) on the Patagonian Shelf (Laptikhovsky and Brickle, 2005). Evidence from genetics (Shaw et al., 2004; Rogers et al., 2006) indicates that toothfish off South America are separated from those in the Antarctic, by a population boundary in the vicinity of the Polar Front in the Antarctic Circumpolar Current (ACC) (Fig. 1). Equatorward of the Polar Front, spawning adults have historically been found only in an area on the Burdwood Bank and western North Scotia Ridge, suggesting that fisheries around the Falkland Islands are supplied by a single discrete population (Laptikhovsky et al., 2006).

Toothfish are slow-growing and live to 50+ years (Ashford, 2001; Horn, 2002). Exceptionally fecund for notothenioids, the females produce up to 250,000 large eggs of ca. 1 mm diameter during spawning (e.g. Nevinski and Kozlov, 2002). The eggs and larvae are pelagic (Evseenko et al., 1995; North, 2002): egg develop-

* Corresponding author. Tel.: +1 757 683 4804; fax: +1 757 683 5293.
E-mail address: jashford@odu.edu (J.R. Ashford).

0165-7836/$ – see front matter © 2012 Elsevier B.V. All rights reserved.
doi:10.1016/j.fishres.2012.01.023

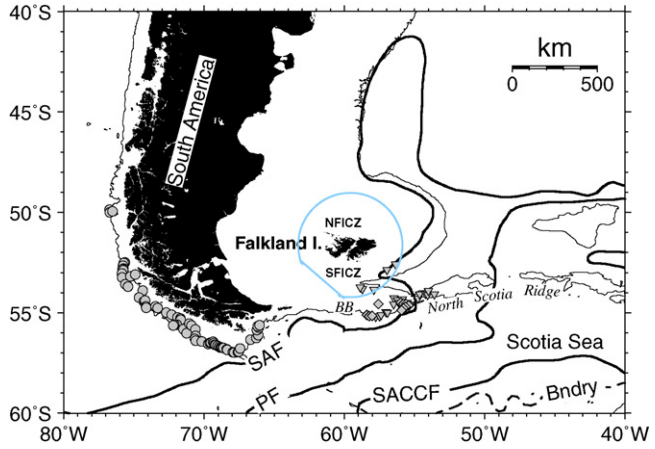

Fig. 1. Study area. Grey circle shows boundary of Falkland Islands Interim Conservation and Management Zone (FICZ). Continuous dark lines mark the mean position of major fronts: SAF, Subantarctic Front; PF, Polar Front; SACCF, Southern Antarctic Circumpolar Current Front; Bndry, southern boundary of the ACC (shown as a dashed line). All fronts after Orsi et al. (1995). Thin lines mark the 2000 m isobar. Abbreviations: BB—Burdwood Bank; NFICZ—North FICZ; SFICZ—South FICZ. Symbols mark drifter release sites corresponding to observed spawning locations off southern Chile (●), and Burdwood Bank of first (▲) and second (⧫) peak spawning sites after Laptikhovsky et al. (2006). Scale bar shows distance at 45° S.

ment lasts up to ca. 90 days (Evseenko et al., 1995) and the larval period spans ca. 230 days (Krusic-Golub et al., 2005). In contrast, juvenile toothfish are negatively buoyant (Eastman, 1993) and move demersally in shelf habitats on scales of only ca. 25 km (Williams et al., 2002). Ontogenetic movement to adult feeding grounds in deeper water along continental slopes (e.g. Agnew et al., 1999) is associated with a change to neutral buoyancy around maturity (Eastman, 1993), which considerably reduces the energy needed to move using currents in the ACC (Ashford et al., 2005). As a result, toothfish life history is marked by important ontogenetic changes in the spatial scales of movement, with the potential for connectivity on scales of 1000s of kilometres through advection of young stages, and also adults.

Circumpolar flow in the Southern Ocean, concentrated in jets associated with the frontal systems in the ACC (e.g. Orsi et al., 1995), passes through a constriction between South America and the Antarctic Peninsula in the Drake Passage. Equatorward of the Polar Front, the Subantarctic Front (SAF) passes south of Cape Horn and Burdwood Bank and north through a trough 2000 m deep in the North Scotia Ridge, to align subsequently with the 2000 m isobath along the Patagonian Shelf slope (Fig. 1) (Arhan et al., 2002). After spawning during May–July, spent female toothfish are found along the slope south of the Falkland Islands (Laptikhovsky et al., 2006), consistent with advection from the Burdwood Bank along the SAF to feeding areas downstream (Ashford et al., 2007). Moreover, larvae found north of the Burdwood Bank during December (North, 2002), 100–200 days after spawning, suggest a connection via advection to juvenile areas exploited by the trawl fishery in the FICZ.

A single discrete population recruiting from the spawning aggregation around Burdwood Bank implies that all fish on the Patagonian Shelf share a common early life history. However, while evidence from otolith chemistry successfully confirmed the population boundary in the vicinity of the Polar Front, it also suggested mixing along the Patagonian Shelf slope between two South American source populations (Ashford et al., 2006). Researchers have recently found a second area with fish spawning in June–July near the SAF but upstream of Burdwood Bank along the south-west shelf-slope off Cape Horn in the Chilean Exclusive Economic Zone (Arana, 2009). If young stages spawned there as well as the Burdwood Bank supply the FICZ, changes in the position and intensity of the SAF, and in spawner abundances at considerable distances from the Falkland Islands, may directly impact local recruitment and subsequent catches in the trawl fishery.

1.2. Testing using a spatially explicit approach

Mounting evidence that fish otoliths record hydrographic exposures (e.g. Bath Martin and Thorrold, 2005; Walther and Thorrold, 2006), combined with the chronology delineated in growth increments, makes otolith chemistry a particularly powerful technique for testing population hypotheses that involve a strong physical component. Previous studies of Patagonian toothfish indicated that the concentration of $Mg\,Ca^{-1}$ laid down in the otolith was related to spatial differences in fish activity, most likely in response to fast-moving currents and eddies. Otolith $Mn\,Ca^{-1}$, on the other hand, appeared related to resuspension or authigenic activity on the Patagonian Shelf, whereas $Sr\,Ca^{-1}$ distinguished growth mediated by temperatures characteristic of different water masses, and $Ba\,Ca^{-1}$ reflected ambient concentrations of dissolved Ba associated with nitrate-fueled production in open water (Ashford et al., 2005). Based on concentrations of these markers, toothfish caught along the Patagonian Shelf re-assigned to region with 94–95% accuracy (Ashford et al., 2005, 2007), and between areas separated at scales of 100s of kilometers along the shelf with a success rate of between 57 and 83% (Ashford et al., 2007).

Exposure to hydrographic properties characteristic of water masses and circulation therefore leaves a record that fish carry with them, which can be used retrospectively to detect connectivity and examine the spatial composition of harvested fish. Despite these physically based response variables, however, fisheries researchers have to date rarely tested hypotheses that incorporate an explicit oceanographic context. Typically, tests are between a null hypothesis of spatial homogeneity in the chemistry laid down in the otolith nuclei, consistent with a common early life history, and an alternative hypothesis of heterogeneity indicative of geographically discrete populations. But fish from several populations mixing in different proportions can also generate spatially heterogeneous distributions, and the approach gives little insight into the complex physical–biological interactions that can underly the population dynamics supporting fishing activity.

A more spatially sensitive approach that incorporates the large-scale circulation is to test hypotheses using particle simulations (e.g. Fach and Klinck, 2006; Thorpe et al., 2007). Inputs and assumptions are rigorously specified but nonetheless, the uncertainties involved in reproducing physical processes often undermine conclusions from these tests. Combined with otolith chemistry, however, particle simulations provide a quantitative means of constructing spatially explicit hypotheses that incorporate the physical circulation, with well-defined predictions of expected trajectories that can be empirically tested against observed distributions in the otolith chemistry (Ashford et al., 2010, 2011b).

In this study therefore, we simulated pelagic transport pathways along the SAF to build spatially explicit predictions that distinguished the rival hypotheses of a single discrete toothfish population versus mixing between fish from two populations, using easily accessible and widely used current velocity fields taken from the OCCAM global circulation model (Webb et al., 1998; Saunders et al., 1999; Webb and de Cuevas, 2003). We used chemistry recorded in the otolith nuclei of toothfish caught in the fishery to test between the predictions, following methodology now well established in the literature (e.g. Dorval et al., 2005; Ashford et al., 2011a). We also measured the chemistry along the otolith edges to examine empirically how recently laid down material varies spatially within the FICZ.

2. Methods and materials

2.1. Developing predictions using particle simulations

To simulate particle transport in the southern Atlantic, we used velocity fields available as output from the global, primitive equation model OCCAM based on the Bryan-Cox ocean general circulation model. The state of the ocean can be modeled with temperature, salinity and the three components of velocity using a momentum equation to give the time change in velocity, and an advection-diffusion equation for changes of temperature and salinity (Webb et al., 1998). In the model, the ocean is divided into a large number of boxes along lines of constant latitude, longitude and depth, forming a three-dimensional grid with average values of ocean properties specified for each box. Topography used by OCCAM is Digital Bathymetric Data Base 5-min (DBDB5) from the U.S. Naval Oceanographic Office which has a 5-min spatial resolution.

Unlike the Bryan-Cox model, OCCAM includes a free surface and is eddy permitting. The version we used has a horizontal resolution of $1/12^\circ \times 1/12^\circ$, the highest available, with 66 depth levels. It is forced by 6 hourly wind stress data from the European Centre for Medium-Range Weather Forecasts, and includes a sea-ice model as described by Askenov (2002). We computed particle trajectories from OCCAM velocity fields using Lagrangian particle tracking with a first-order accurate scheme. The scheme integrates $d\vec{x}/dt = \vec{u}(\vec{x}, t)$ where the left-hand side is the rate of change of the particle location over time and the right-hand side is the velocity field that changes in space and time, provided monthly by OCCAM. The right-hand side is computed by interpolating linearly in time and space between mean OCCAM velocity fields. We chose a very small time step (dt = 1 min) making this particle tracking scheme comparable to a second-order accurate scheme and ensuring appropriate accuracy.

Using the Lagrangian tracking code, we simulated the trajectories of particles released from observed spawning locations for Patagonian toothfish on the Burdwood Bank (▲) and western North Scotia Ridge (♦) and the south-western slope off Chile (●) (Fig. 1). Pelagic toothfish eggs and larvae have been found in surface waters (North, 2002) and therefore particles were tracked in the surface layer of the model. To catch seasonal transport changes during and after the time of observed spawning periods (May and July for Burdwood Bank, Laptikovsky et al. (2006); and June to July for the south-western slope off Chile; Arana, 2009), they were released in monthly cohorts on Day 15 of each month from May to November. Simulations were repeated for different years (1996–2000) to assess interannual variability. Because the pelagic period for toothfish consists of 90 days of egg development and a larval period of 230 days, particles were always tracked for 320 days after release.

2.2. Testing predictions using otolith chemistry

Scientific observers placed on commercial trawlers fishing in the FICZ (Fig. 1) sampled juvenile toothfish taken at depths of 200–250 m during austral winter–spring of 2001 to the north (n = 42) and south (n = 36) of the Falkland Islands. At each sampling area, toothfish were taken from the catch, and total length, weight, sex and maturity stages recorded for each fish. Otoliths were extracted using plastic forceps, and stored dry in paper envelopes. We estimated age for each fish using techniques given in Ashford et al. (2007), and measured concentrations of trace and minor elements using the Finnegan Mat Element 2 double-focusing sector-field Inductively Coupled Plasma Mass Spectrometer (ICP-MS) located at the Laboratory for Isotope and Trace Element Research (LITER) at Old Dominion University. Samples were introduced on petrographic slides into ICP in automated sequence (Chen et al., 2000) using a combination of laser ablation by a New Wave Research EO LUV 266 laser ablation system and solution nebulization using a PFA microflow nebulizer (50 μL min^{-1}, Elemental Scientific Inc., Omaha). Full details are given in Ashford et al. (2007).

For quality control, we used dissolved otolith reference material obtained from the National Research Council of Canada, and a randomized blocks design to control for operational variability in the laser-ICP-MS, in which otoliths from each sampling area, considered a fixed treatment, were randomly assigned to each petrographic slide as the blocking factor considered randomly drawn. To sample material laid down during early life, we placed a grid raster type 150 μm × 200 μm over the nucleus to include the primordium and material surrounding the primordium, with a laser beam of diameter 20 μm, frequency at 10 Hz, and power at 60%, traveling ca. 900 μm at 6 μm s^{-1} and giving a predicted mean crater width of 17 μm, and crater depth of approximately 100 μm (Jones and Chen, 2003, Eq. (3)). Material was analyzed for ^{48}Ca, ^{25}Mg, ^{55}Mn, ^{88}Sr, and ^{138}Ba, with counts averaged over the length of the line for each marker, and reported as ratios to ^{48}Ca, the internal standard. We also examined material laid down just prior to capture, by placing a line raster type along the proximo-dorsal edge of the otolith corresponding to approximately the 2001 annulus, and using the same settings.

Multivariate outliers were identified for both edge and nucleus data by plotting robust squared Mahalanobis distances of the residuals (D_i^2) against the corresponding quantiles (Q–Q plot) of the chi-square distribution (Khattree and Naik, 1999). Based on tests using Mardia's multivariate skewness and kurtosis measures (α = 0.05), and Q–Q plots of squared Mahalanobis distances (d_i^2), edge and nucleus data conformed to multivariate normality after variance-stabilizing transformation using the ladder of powers (Kuehl, 1994, p. 121; Ashford et al., 2007). The transformations for the nucleus data were $y^{-0.8}$ for Mg Ca^{-1}, y^{-1} for Mn Ca^{-1}, $y^{0.5}$ for Sr Ca^{-1}, and y^{-1} for Ba Ca^{-1}. For edge data, they were $y^{-0.5}$ for Mg Ca^{-1}, ln(y) for Mn Ca^{-1}, y^{-1} for Sr Ca^{-1}, and y^{-3} for Ba Ca^{-1}.

Variance–covariance matrices were still not equal according to Bartlett's modification (edge data: χ^2 = 39.1, df = 15, $p > \chi^2$ = 0.0006), so multivariate ANOVA was inappropriate, and we used univariate ANOVA to examine differences. The nucleus data showed equality of variances for all transformed Me Ca^{-1} ratios (F_{max} test; α = 0.01), and residuals were normally distributed (Kolmogorov–Smirnov test; α = 0.05). Residuals for edge data showed homogeneity of variances (F_{max} test; α = 0.01), except Sr Ca^{-1} which departed marginally from homogeneity (F_{max} test = 2.85; $F_{max\ 0.01,2,35}$ = 2.5). All residuals were distributed normally except Mn Ca^{-1} in fish caught north of the Falkland Islands (Kolmogorov–Smirnov test; p = 0.047).

Effects due to age and sex were tested for both nucleus and edge data for each Me Ca^{-1} using ANCOVA models with age as a covariate and sex as a blocking factor. Interaction effects were insignificant. For the nucleus data, there was no temporal effect for the southern FICZ, but we found some evidence in fish from the northern FICZ of temporal trends for Mg Ca^{-1} (ANCOVA; p = 0.023) and Ba Ca^{-1} (ANCOVA; p = 0.005). However, age accounted for little variance (R^2_{mg} = 14.6%; R^2_{ba} = 17.2%) and the effect was due to data points at the extremes of the distribution. For edge data, Sr Ca^{-1} showed no significant effects due to sex and the block was dropped; Ba Ca^{-1} showed no significant effect due to age or sex, so both covariate and block terms were dropped from the model. For both edge and nucleus data, we used Student t statistics t_0 calculated for each comparison within a family of four comparisons, and adjusted for the experiment-wise α-level using Bonferroni t with a critical value of $t_{\alpha_e/2,k,\nu}$ for k two-sided comparisons and ν degrees of freedom.

To quantify differences in otolith chemistry laid down between sampling areas, we estimated contrasts for each edge Me Ca^{-1} ratio, with standard errors and confidence intervals, and comparison-wise power $1-\beta > 0.99$ (Kuehl, 1994). We calculated the number of standard deviations (SD) between the means, a function of the contrast relative to within-area variability, as an index of relative power to resolve areas (Ashford et al., 2007).

Because variance–covariance matrices were not equal, we could not use Canonical Discriminant Analysis, and we used non-metric multidimensional scaling (nMDS) instead to illustrate graphically the differences found (Kruskal and Wish, 1978; Schiffman et al., 1981). Transformed edge data were detrended for age. Because the variables had different absolute magnitudes and ranges, they were standardized to the same scale for both edge and nucleus data. Constructing a dissimilarity matrix based on Euclidean distances, we created two-dimensional projections of distance between individual fish using convergence criteria of stress < 0.01.

3. Results

3.1. Predictions from particle simulations

Particles released from the western North Scotia Ridge during the spawning season were entrained directly into the SAF and swept rapidly north, away from the Falkland Islands and eventually out into the Atlantic. Trajectories are illustrated in Fig. 2 for exemplar year 1998. Particles released directly from Burdwood Bank were often not entrained in the fast flowing SAF currents until much later. Instead, some were retained initially in eddy systems south of the bank, to its north, and between it and the southern Patagonian Shelf; and remained 100–200 days in eddy systems south and east of the Falkland Islands (Fig. 2b and c). In contrast, when particles were released in the months after the spawning season, they were not retained as long: by 100 days, almost all were entrained in the SAF well north of the Falkland Islands. Similarly, even during the spawning season, particles released on the far north-east side of Burdwood Bank were also quickly entrained into the SAF, although less rapidly than those from the North Scotia Ridge.

Nevertheless, many of the particles released from the Burdwood Bank during the spawning season reached the FICZ. On average between May and July, 15–17% were present in the southern FICZ after 50 days, 7–11% after 100 days, and up to 2% remained after 300 days (Table 1a). However, much fewer reached the northern FICZ with an average of 0.5–3% present after 100 days, and none after 250 days. The eddy systems persisted throughout the years simulated but their extent and exact location varied from year to year: in years when the eddy forming south of Burdwood Bank grew more persistent, it enabled particles to stay in the area for up to 250 days, before becoming entrained in a second eddy north of Burdwood Bank (Fig. 2c). In 1998 in particular, 8–10% of the particles released in June and July were located in the southern FICZ after 300 days. Even in 1998 however, no particles were present in the northern FICZ after 250 days. These simulations indicated that the large-scale circulation could retain early stages south of the Falkland Islands during the pelagic period after spawning and transport them to the southern Patagonian Shelf. By the time they reached areas north of the islands, however, the young fish were already entrained in the SAF and unlikely to be deposited over the shelf.

Simulations from the shelf slope south-west of Cape Horn showed a different pattern. Some particles were retained over the shelf south of Tierra del Fuego, mainly because of stable eddy systems forming at the shelf edge. These systems changed position slightly with season but persisted during the entire simulation period from May to November (Fig. 3). However, many particles from the south-western slope passed very close by the Falkland

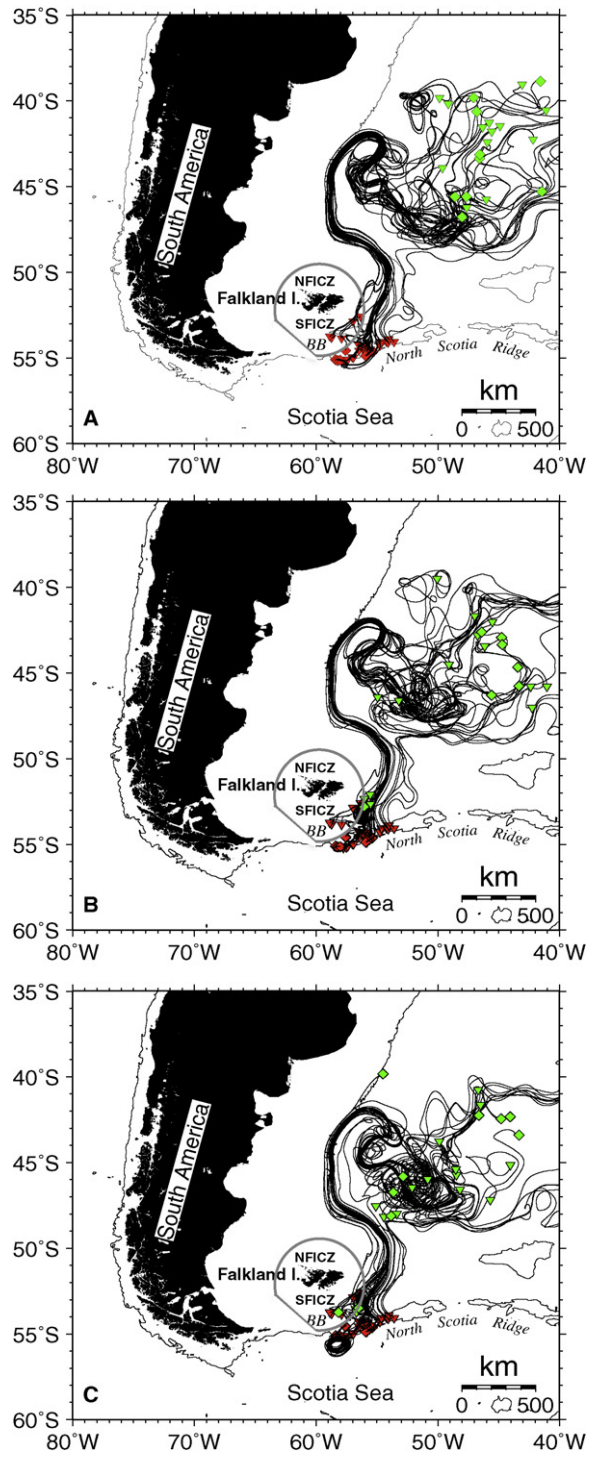

Fig. 2. Simulations of surface particle trajectories released from Burdwood Bank of first (red, ▲) and second (red, ♦) peak spawning sites in (A) May, (B) June, and (C) July 1998 and tracked for 320 days (endpoints green (▲) and (♦), respectively). Grey circle shows boundary of Falkland Islands Interim Conservation and Management Zone (FICZ). Thin lines mark the 2000 m isobar. Abbreviations: BB—Burdwood Bank; NFICZ—North FICZ; SFICZ—South FICZ. Ocean velocity fields taken from OCCAM (Webb et al., 1998; Saunders et al., 1999; Webb and de Cuevas, 2003); the mode output (run 401) has a horizontal resolution of 1/12° × 1/12° and is forced by the European Centre for Medium-Range Weather Forecasts 6 hourly wind stress data. Scale bars shows distance at 45° S.

Table 1
Mean percentage (range) of drifters released between May and June 1996–2000 from (a) Burdwood Bank and (b) southern Chile, present in the northern and southern FICZ at 50–300 days.

(a)

Month	Destination	Mean % in FICZ at day				
		50	100	200	250	300
May	North	2.6 (0–5)	3 (0–8)	0	0	0
	South	17 (0–38.5)	11 (0–26)	1.5 (0–5)	1.5 (0–5)	1.5 (0–5)
June	North	1 (0–2.6)	1 (0–5)	1 (0–5)	0	0
	South	16 (5–26)	7 (0–23)	0.5 (0–2.5)	1 (0–5)	1.5 (0–8)
July	North	3.6 (0–13)	0.5 (0–2.6)	0	0	0
	South	15 (5–20.5)	11 (5–15)	3 (0–10)	1.5 (0–8)	2 (0–10)

(b)

Month	Destination	% in FICZ at day				
		50	100	200	250	300
May	North	1.8 (0–4)	7.5 (3–11)	13 (6–22)	3 (1.5–6)	1.5 (0–3)
	South	17 (4.5–31)	27 (16–44)	5 (0–10)	2 (0–3)	2.3 (0–6)
June	North	0.8 (0–4)	10 (1.5–25)	10 (6–17)	2 (0–6)	1.8 (0–4)
	South	14.5 (3–26)	22.5 (10–40)	3 (0–4)	3 (0–10)	2 (0–4)
July	North	2.4 (0–4)	12 (3–24)	9 (4–19)	3.5 (1.5–9)	3.5(3.5–10)
	South	11 (3–25)	28.5 (15–46)	3.3 (1.5–10)	3.5(1.5–12)	3.5(1.5–10)

Islands, following transport pathways through both the northern and southern FICZ. Some crossed on to the shelf near Tierra del Fuego (Fig. 3), west and east of Staten Island: of these, most were advected quickly northwards but some took as long as 320 days, reaching the FICZ coinciding with the end of their pelagic period. Other particles followed the SAF before moving onto the shelf west and north of Burdwood Bank. However, these particles were transported much more quickly and arrived south of the Falkland Islands by 50–100 days before being entrained northwards in the fast SAF currents. Overall, more particles from south-west of Cape Horn reached the south FICZ than the north: on average between May and July, 22.5–28.5% were present in the south after 100 days, compared to 7.5–12% for the north (Table 1b). Nevertheless, the disparity in those remaining in each area reduced steadily over 300 days, to an average of 2–3.5% in the south after 300 days and 1.5–3.5% in the north.

Variability between years was important, but affected advection from the two spawning areas differentially. The proportion of particles released from south-west of Cape Horn after 300 days reached a maximum of 10% in both the northern and southern FICZ; however, this maximum occurred in 1996, and did not coincide with the one in 1998 from Burdwood Bank to the south FICZ. After the spawning season, fewer particles were retained off Cape Horn, and transport to the FICZ was faster, so that almost all were advected northwards out of the FICZ before 320 days.

3.2. Tests using otolith chemistry

The mean age of fish taken north of the Falkland Islands was 5.3 (SD ± 1.8) years, corresponding to the cohort spawned in 1996, whereas the mean age of fish taken south of the islands was 3.2 (SD ± 1.00) years, corresponding to the cohort spawned in 1998. Fish from the north FICZ showed strong differences from those from the south FICZ in their otolith chemistry as well. In material laid down in the nuclei during early life, northern fish had lower mean concentrations of Mg Ca^{-1} than southern fish (mean ± SD; $\bar{x}_{NFICZ} = 120.5 \pm 9.5\,\mu$mol mol^{-1}; $\bar{x}_{SFICZ} = 163.1 \pm 8.6\,\mu$mol mol^{-1}) and higher Mn Ca^{-1} ($\bar{x}_{NFICZ} = 3.84 \pm 0.19\,\mu$mol mol^{-1}; $\bar{x}_{SFICZ} = 2.7 \pm 0.09\,\mu$mol mol^{-1}). Northern fish also had lower mean concentrations of Sr Ca^{-1} than southern fish ($\bar{x}_{NFICZ} = 868 \pm 24\,\mu$mol mol^{-1}; $\bar{x}_{SFICZ} = 1040 \pm 41.2\,\mu$mol mol^{-1}) and higher Ba Ca^{-1} ($\bar{x}_{NFICZ} = 0.66 \pm 0.18\,\mu$mol mol^{-1}; $\bar{x}_{SFICZ} = 0.55 \pm 0.04\,\mu$mol mol^{-1}). These differences were significant for Mg Ca^{-1}, Mn Ca^{-1} and Sr Ca^{-1} (Table 2), exceeding the Bonferroni t critical value ($t_{\alpha_e/2,4,79} = 2.54$), but not for Ba Ca^{-1} (ANOVA; d.f. = 1, 79; $F = 0.54$; $p = 0.46$). Multidimensional scaling illustrated the differences found (Fig. 4) and indicated that, while fish with similar chemistry were found north and south of the islands consistent with origin from southern Chile, the heterogeneity was generated by fish in the south with nucleus chemistry that was not found to the north, consistent with predicted trajectories from Burdwood Bank.

The chemistry at the otolith edge, laid down during the year prior to capture, also showed strong heterogeneity. Fish north of the Falkland Islands had lower mean concentrations of Mg Ca^{-1} than fish to the south ($\bar{x}_{NFICZ} = 66.9 \pm 2.9\,\mu$mol mol^{-1}; $\bar{x}_{SFICZ} = 139.6 \pm 13.8\,\mu$mol mol^{-1}) and lower Mn Ca^{-1} ($\bar{x}_{NFICZ} = 0.34 \pm 0.04\,\mu$mol mol^{-1}; $\bar{x}_{SFICZ} = 0.77 \pm 0.14\,\mu$mol mol^{-1}). Northern fish showed higher mean concentrations of Sr Ca^{-1} at the otolith edge than southern fish ($\bar{x}_{NFICZ} = 2548 \pm 107\,\mu$mol mol^{-1}; $\bar{x}_{SFICZ} = 1644 \pm 45\,\mu$mol mol^{-1}), and higher Ba Ca^{-1} ($\bar{x}_{NFICZ} = 0.90 \pm 0.04\,\mu$mol mol^{-1}; $\bar{x}_{SFICZ} = 0.55 \pm 0.02\,\mu$mol mol^{-1}). Multidimensional scaling illustrated the strong separation between NFICZ and SFICZ (Fig. 5). The differences were significant for all element ratios (Table 3), exceeding the Bonferroni t critical value ($t_{\alpha_e/2,4,79} = 2.54$), and contrasts between north and south of the FICZ estimated from the transformed data were large (Table 4), ranging between one full SD for Mn Ca^{-1}, over 1.7 SD for Mg Ca^{-1} and Ba Ca^{-1}, to nearly 1.9 SD for Sr Ca^{-1}. These data indicated strong differences in environmental exposure between fish north and south of the Falkland Islands.

Table 2
Nucleus chemistry: mean square estimates from 1-way ANOVA for Mg Ca^{-1}, Mn Ca^{-1}, Sr Ca^{-1}, and Ba Ca^{-1}, between northern and southern FICZ.

	df	Mg Ca^{-1}	Mn Ca^{-1}	Sr Ca^{-1}	Ba Ca^{-1}
Sampling area	1	0.00425***	1.267***	5.61×10^{-7}***	0.0086
Residual	74	0.00019	0.049	0.43×10^{-7}	0.0157

*$p < 0.05$.
**$p < 0.01$.
*** $p < 0.001$.

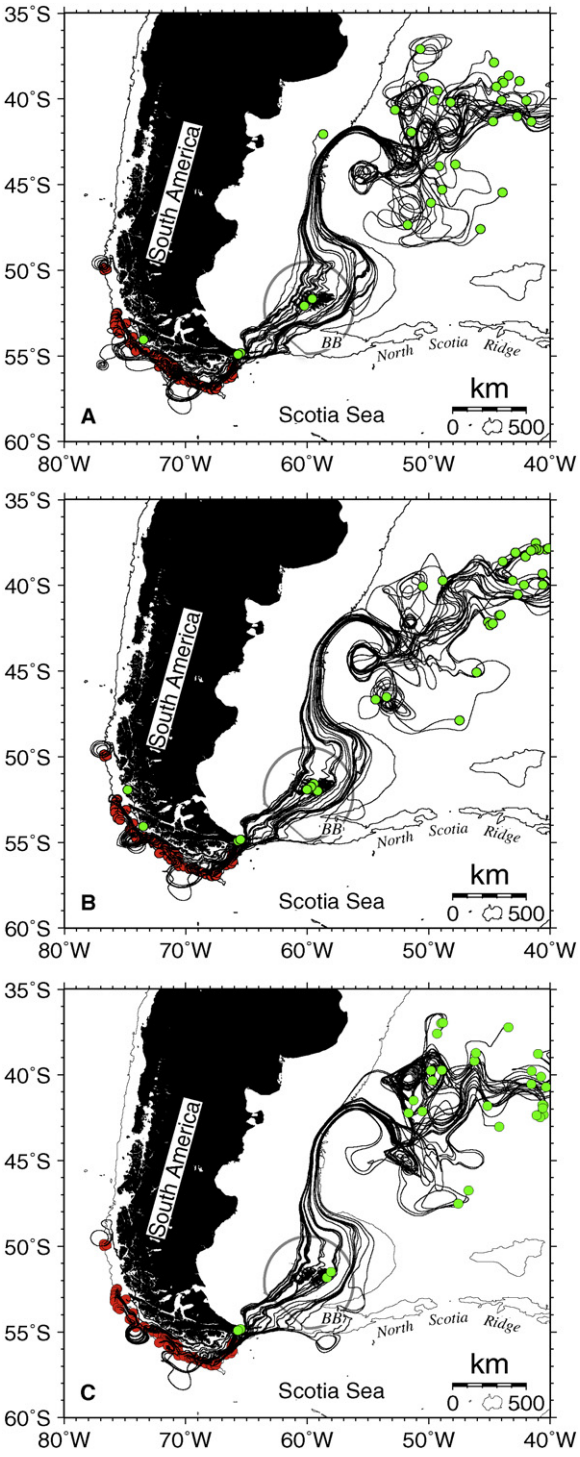

Fig. 3. Simulations of surface particle trajectories released from south-west of Cape Horn (red, ●) in (A) May, (B) June, (C) July 1998 and tracked for 320 days (endpoints green, ●). Grey circle shows boundary of Falkland Islands Interim Conservation and Management Zone (FICZ). Thin lines mark the 2000 m isobar. BB—Burdwood Bank. Scale bar shows distance at 45° S.

4. Discussion

4.1. A single population does not account for the data

By pairing particle-tracking simulations and otolith chemistry, we created spatially explicit hypotheses and tested them empirically using response variables that reflected hydrographic properties. Strong heterogeneity in the nucleus chemistry of fish

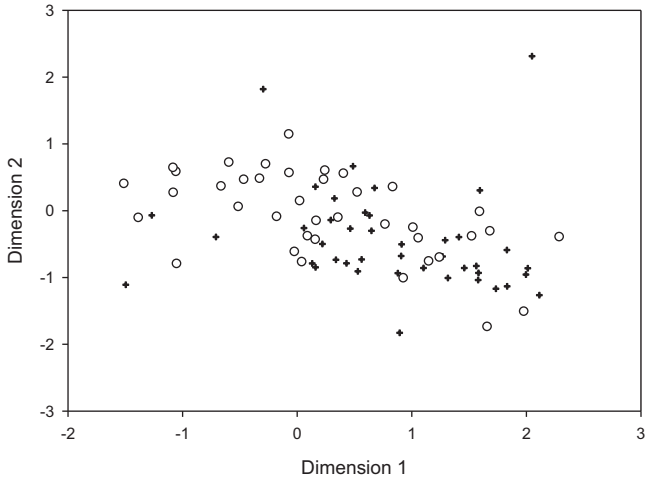

Fig. 4. Otolith nucleus chemistry, using non-metric multi-dimensional scaling (nMDS) based on Euclidean distances. Symbols: NFICZ (+), SFICZ (◯). Note: the axes in nMDS do not bear a direct relation to ordinations.

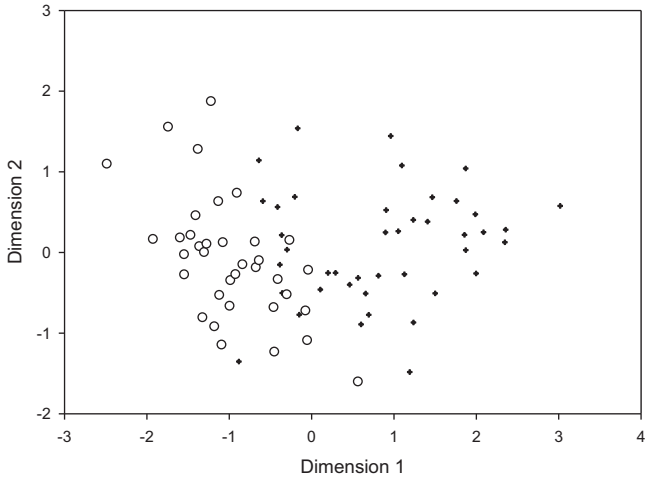

Fig. 5. Otolith edge chemistry, using non-metric multi-dimensional scaling (nMDS) based on Euclidean distances. Symbols: NFICZ (+), SFICZ (◯). Note: the axes in nMDS do not bear a direct relation to ordinations.

Table 3
Edge chemistry: mean square estimates from: (a) 1-way ANCOVA for Mg Ca^{-1} and Mn Ca^{-1}, using age as covariate and blocked by sex; (b) 1-way ANCOVA for Sr Ca^{-1}, using age as covariate; (c) 1-way ANOVA for Ba Ca^{-1}, between northern and southern FICZ.

(a)	df	Mg Ca^{-1}	Mn Ca^{-1}
Sampling area	1	0.00117***	0.416*
Age	1	0.00053**	0.896**
Sex	1	0.00030*	0.389*
Residual	74	0.00004	0.086

(b)	df	Sr Ca^{-1}
Sampling area	1	394***
Age	1	639***
Residual	75	23

(c)	df	Ba Ca^{-1}
Sampling area	1	0.912***
Residual	76	0.016

* $p < 0.05$.
** $p < 0.01$.
*** $p < 0.001$.

Table 4
Contrasts between sampling areas ($C = \bar{x}_{NFICZ} - \bar{x}_{SFICZ}$), using chemistry from otolith edges of juvenile *Dissostichus eleginoides*. s_c—SE of the contrast; CI—confidence interval; SD—standard deviation. FICZ—Falkland Islands Inner Conservation Zone; NFICZ—north FICZ; SFICZ—south FICZ.

Me/Ca	C	s_c	95% CI Upper/lower	No. SD
Mg/Ca	0.013	0.0015	0.016/0.010	1.71
Mn/Ca	0.332	0.0667	0.464/0.200	1.02
Sr/Ca	9.6	1.081	10.7/8.5	1.88
Ba/Ca	0.217	0.0289	0.0274/0.1600	1.75

caught north and south of the Falkland Islands discounted the hypothesis of a single population with a spawning area on Burdwood Bank that exclusively supplies the trawl fishery around the Falkland Islands. Instead, our data was consistent with the alternative hypothesis that spawning areas off both southern Chile and the Burdwood Bank supply the trawl fishery, structuring assemblages of juvenile fish through a combination of large-scale transport and retention in eddies south of the Falkland Islands.

Like all global circulation models, OCCAM has certain strengths and weaknesses associated with its ability to resolve the flow in different areas of the global ocean. Validated for the Scotia Sea and the Weddell Sea regions, it has been found to represent the circulation in the Drake Passage reasonably well (Thorpe et al., 2005) and has been used successfully in other particle tracking studies in the Southern Ocean (Ward et al., 2002; Murphy et al., 2004; Thorpe et al., 2007; Ashford et al., 2010, 2011b). Although the resolution used here ($1/12^\circ \times 1/12^\circ$) has been found to produce flow with high mesoscale variability that represents the Southern ACC Front (Fig. 1) and the Weddell Front (both in the Antarctic outside the current study area) as too weak, it resolves the flow of the SAF according to observations (Renner et al., 2009). Model resolution is not fine enough to resolve small-scale features like coastal currents around islands and landmasses that may also retain particles, and the simulations do not include any fish behavior. However, the empirical data validated the simulations, indicating that transport by the large-scale circulation accounted for the distributions of nucleus chemistry, without need to invoke either small-scale processes or behavior.

Moreover, consistent with influx of water predicted by the simulations, the chemistry laid down along the otolith edges just before capture also showed strong heterogeneity. Physical transport that supplies the trawl fishery in the FICZ from spawning areas around Cape Horn and Burdwood Bank, appears to influence the properties of shelf water as well. South of the Falkland Islands, fish showed high $Mg\,Ca^{-1}$ consistent with activity previously associated with circulation between the Burdwood Bank and southern Patagonian Shelf, while $Mn\,Ca^{-1}$, at lower concentrations north of the Falkland Islands, was consistent with depletion found previously along the northern slope (Ashford et al., 2005, 2007). $Sr\,Ca^{-1}$, linked previously to water temperature, and $Ba\,Ca^{-1}$, linked to nitrate-fuelled production in the ACC, were depleted in both sampling areas; however, concentrations of both element ratios remained higher north of the Falkland Islands, consistent with simulations showing influx of water over the shelf from oceanic areas in the ACC.

Thus, the simulations allowed us to explore each population hypothesis for sharply contrasting and mutually exclusive predictions (Popper, 1959). Because these were spatially specific, they could be examined in a cost-effective and powerful design that minimized sampling effort and laboratory analysis while simultaneously enhancing discrimination between the competing hypotheses. Consequently, we were able to test between two spatially sophisticated scenarios with a power greater than 95%, using otoliths from only 78 fish divided between two treatments. Beyond these logistical and statistical advantages, the spatially explicit approach gave rich insight into the ways physical forcing

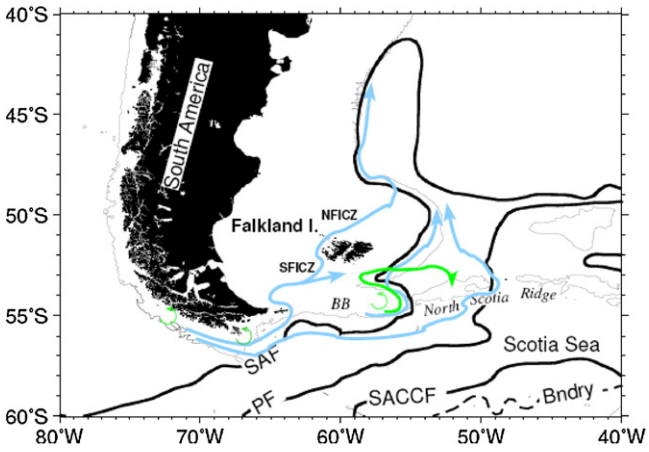

Fig. 6. Life history cycle hypothesized for toothfish off southern Chile and on the Patagonian Shelf, showing trajectories (i) retaining membership in spawning populations (in green) and (ii) leading to vagrancy and loss of population membership (in blue). Note crossing over south of the Falkland Islands from a trajectory from southern Chile to the membership trajectory for Burdwood Bank. Thin lines mark the 2000 m isobar. Abbreviations: BB—Burdwood Bank; NFICZ—North FICZ; SFICZ—South FICZ.

potentially influences the abundance and distribution of fish available to the fishery, which in turn can be used to develop new hypotheses to incorporate complex interactions between the large-scale circulation and life history.

4.2. A spatially explicit hypothesis incorporating hydrography and life history

Physical features are potentially key to understanding the population processes that structure toothfish assemblages. Our simulations suggest that stable eddy systems off southern Chile and Burdwood Bank can promote self-recruitment by retention, while those south and east of the Falkland Islands can also retain young fish long enough for them to settle as juveniles in the southern FICZ. Similarly stable eddies increase the residence time of entrained water north of the Falkland islands, often corresponding to areas of marine life accumulation (e.g. Glorioso, 2002; Upton and Shaw, 2002) As a result, water transported and entrained in these eddies may not only structure assemblages of juveniles by supplying early stages from southern Chile, but also position them where production and marine life accumulation promote food availability, reinforcing the limited movement subsequently shown during the demersal juvenile stage.

Once toothfish become neutrally buoyant at maturity, however, the large-scale circulation in the north FICZ is northwards, towards the northern shelf-slope. Ontogenetic movement to depth exposes fish arriving on the slope to fast northward flow along the SAF (Fig. 6), as well as Antarctic Intermediate Water (AAIW) where it sinks north of the Polar Front (Arhan et al., 2002). In the south FICZ, ontogenetic movement to depth has a similar effect initially, but Lower Circumpolar Deep Water occupies the deep layer below AAIW over the Falkland Plateau, where it is associated with southward flow (Arhan et al., 2002). Unlike adult toothfish to the north, those moving to depth from the south FICZ would potentially be advected toward the North Scotia Ridge. Distributions of nucleus chemistry in adults along the northern and southern Patagonian shelf slope support this divergence (Ashford et al., 2006; Fig. 7), showing extensive heterogeneity between sampling areas north of the Falkland Islands and those to the east and south.

Interactions between the large-scale circulation and life history may help account for other features of population distribution. Along the North Scotia Ridge, an anomalous low-oxygen type of

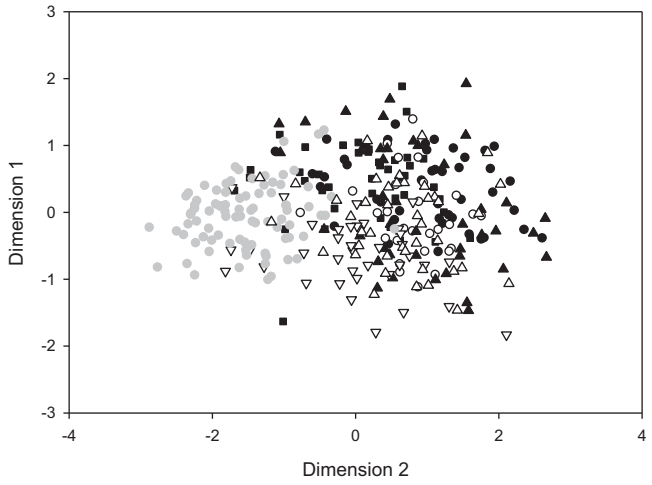

Fig. 7. Relationships between adult Patagonian toothfish in the south-western Atlantic Ocean, using non-metric multidimensional scaling based on Euclidean distances obtained from nucleus chemistry. Data from Ashford et al. (2006, Fig. 3; sampling areas shown in Fig. 1). (a) International waters (○); (b) North FOCZ (△); (c) East FOCZ (■); (d) Burdwood Bank/South FOCZ (●); (e) western North Scotia Ridge (▲); (f) eastern North Scotia Ridge (inverted, △). Data from South Georgia shown in grey for reference.

Upper Circumpolar Deep Water (UCDW) from the Chilean continental slope is found at stations along the equatorward flank of the Polar Front (Naveiro-Garabato et al., 2002), downstream of southern Chile where warm-core eddies forming on the poleward side of the SAF follow a trajectory aligned with the ACC flow (Sprintall, 2003). Adult movement off southern Chile and exposure to warm-core eddy activity, with subsequent transport along the ACC (Fig. 6), would explain similarities in nucleus chemistry of fish caught along the eastern North Scotia Ridge to those along the slope north of the Falkland Islands (Ashford et al., 2006). Moreover, the Polar Front divides into two full-depth currents north of the North Scotia Ridge, providing a transport pathway along the western branch that connects to the northern slope of the Patagonian Shelf. The highest velocities in the western branch are at depths of 1500 m (Arhan et al., 2002), within the depth range targeted by longliners fishing on adults.

4.3. Complex population structure on the Patagonian Shelf

Spawning aggregations off southern Chile and Burdwood Bank that supply juvenile feeding areas in the FICZ are consistent with life history cycles in which life stages take advantage of different habitats (e.g. Harden Jones, 1968). For a population to persist, however, at least some fish must close their life cycle by returning to spawn successfully. In this way, a life cycle can be considered as a continuity solution linking areas within a physical system that imposes spatial constraints (Sinclair and Iles, 1989). For the juvenile areas in the FICZ to be part of the solution for either population, however, there must be at least one trajectory by which the juveniles can return as spawning adults to Cape Horn and the Burdwood Bank, upstream in the ACC.

Deep southward currents over the Falkland Plateau may represent such a trajectory, linking adult feeding grounds on the southern Patagonian slope to spawning areas around Burdwood Bank. However, it is more difficult to see how fish advected north of the Falkland Islands can return to spawning areas south of Cape Horn. Adult toothfish are not physiologically capable of sustained counter-current migration and, although neutrally buoyant, there are no return pathways in the large-scale circulation. Instead, population persistence may depend on the small proportion of young fish retained off southern Chile, which subsequently supply juvenile areas on the shelf south of Tierra del Fuego and return to depth as adults to feed and spawn along the continental slope (Fig. 6). Only fish that are positioned to continue through their life cycle in this way remain as members of the population. In contrast, juvenile areas in the FICZ reflect the prevailing transport of larvae (e.g. Beck et al., 2003), but fish advected there are lost from the population off southern Chile: even though they can survive and grow successfully, they become non-breeding vagrants (Sinclair, 1988). Similarly, fish advected from southern Chile to the eastern North Scotia Ridge are probably rendered incapable of returning to their parental spawning areas; instead, they are also eventually transported to the northern slope of the Patagonian Shelf along the western branch of the Polar Front.

However, transport trajectories from southern Chile intersected those from the Burdwood Bank in juvenile areas south of the Falkland Islands, potentially enabling some fish to switch between populations. A small proportion of adults along the southern shelf-slope, and on the Burdwood Bank and western North Scotia Ridge (Ashford et al., 2006), showed nucleus chemistry suggesting immigration from southern Chile, consistent with ontogenetic movement from the southern FICZ and subsequent transport southwards to the North Scotia Ridge. As a result, forcing around Cape Horn may not only drive the distribution and abundance of juveniles in the FICZ, but also subsidize the Burdwood Bank population if immigrants spawn successfully.

These results illustrate the importance of distinguishing areas critical to the life cycle trajectory necessary for population membership from those that represent dead-ends (Sinclair and Iles, 1989) or pathways supporting immigration (Pulliam, 1988). In the case of toothfish, spawning off southern Chile supplies the trawl fishery in the FICZ. However, juvenile areas north of the Falkland Islands may be unimportant to the persistence of any population, whereas those south of the Falkland Islands form a critical link in the life cycle trajectory associated with spawning on the Burdwood Bank. The southern areas, moreover, may be important by supporting immigration: if population persistence on the Burdwood Bank relies on a subsidy from southern Chile to offset mortality, declines in supply may quickly lead to extinction. If so, local variability in physical processes and distributions of toothfish south of Cape Horn may have cascading impacts on much larger spatial scales, destabilizing fisheries downstream. Particle tracking simulations can be used to examine these effects, generating predictions that can be empirically tested using otolith chemistry. By linking fish explicitly to their physical environment, the two techniques can help elucidate how hydrography and life history interact to structure the fish assemblages on which marine fisheries depend.

Acknowledgements

We would like to thank the fishery observers of the Falkland Island Fisheries Dept. who collected the samples, and several current and former colleagues at Old Dominion University: Christian Reiss, now at the National Marine Fisheries Service's Antarctic Marine Living Resources Program, for many invaluable insights; Dayanand Naik, of the Mathematics and Statistics Dept., for advice on statistical methodology; Zhongxing Chen, now at the Dept. of Earth and Planetary Sciences at Harvard University, for expertise in ICPMS techniques; Erick Larson, formerly at CQFE, who prepared the otoliths and ran the ICPMS assays; and Jason Schaffler at CQFE for valuable comments on the manuscript. The Institute of Marine Sciences at the Middle East Technical University provided computer facilities and resources. Funding was from the Falkland Islands Government and the United States National Science Foundation (project no. NSF OPP-0338294).

References

Agnew, D.J., Heaps, L., Jones, C., Watson, A., Berkieta, K., Pearce, J., 1999. Depth distribution and spawning pattern of *Dissostichus eleginoides* at South Georgia. CCAMLR Sci. 6, 19–36.

Almany, G.R., Berumen, M.L., Thorrold, S.R., Planes, S., Jones, G.P., 2007. Local replenishment of coral reef fish populations in a marine reserve. Science 316, 742–744.

Arana, P., 2009. Reproductive aspects of the Patagonian toothfish (*Dissostichus eleginoides*) off southern Chile. Lat. Am. J. Aquat. Res. 37 (3), 381–394.

Arhan, M., Naveira Garabato, A.C., Heywood, K.J., Stevens, D.P., 2002. The Antarctic Circumpolar Current between the Falkland Islands and South Georgia. J. Phys. Oceanogr. 32, 1914–1931.

Ashford, J.R., 2001. In support of a rationally managed fishery: age and growth in Patagonian toothfish (Dissostichus eleginoides). PhD dissertation. Old Dominion University, Norfolk, VA.

Ashford, J.R., Jones, C.M., Hofmann, E.E., Everson, I., Duhamel, G., Moreno, C., Williams, R., 2005. Can otolith elemental signatures record the capture site of Patagonian toothfish (*Dissostichus eleginoides*), a fully marine fish in the Southern Ocean? Can. J. Fish. Aquat. Sci. 62, 2832–2840.

Ashford, J.R., Arkhipkin, A.I., Jones, C.M., 2006. Can the chemistry of otolith nuclei determine population structure of Patagonian toothfish (*Dissostichus eleginoides*)? J. Fish. Biol. 69, 708–721.

Ashford, J.R., Arkhipkin, A.I., Jones, C.M., 2007. Otolith chemistry detects frontal systems in the Antarctic Circumpolar Current. Mar. Ecol. Prog. Ser. 351, 249–260.

Ashford, J.R., La Mesa, M., Fach, B.A., Jones, C., Everson, I., 2010. Testing early life connectivity using otolith chemistry and particle-tracking simulations. Can. J. Fish. Aquat. Sci. 67, 1303–1315.

Ashford, J.R., Jones, C.M., Hofmann, E.E., Everson, I., Duhamel, G., Moreno, C., 2011a. Otolith chemistry indicates population structuring by the Antarctic Circumpolar Current. Can. J. Fish. Aquat. Sci. 65 (2), 135–146.

Ashford, J.R., Serra, R., Saavedra, J.C., Letelier, J., 2011b. Otolith chemistry indicates large-scale connectivity in Chilean jack mackerel (*Trachurus murphyi*), a highly mobile species in the Southern Pacific Ocean. Fish. Res. 107, 291–299.

Askenov, Y., 2002. The Sea Ice-Ocean global coupled ARCICE Project Report Part 1: description of dynamical-thermodynamical sea ice model. Southampton Oceanography Centre Research & Consultancy report 103, Southampton, United Kingdom, 83 pp.

Bath Martin, G., Thorrold, S.R., 2005. Temperature and salinity effects on magnesium, manganese and barium incorporation in otoliths of larval and early juvenile spot *Leiostomus xanthurus*. Mar. Ecol. Prog. Ser. 293, 223–232.

Beck, M.W., Heck, K.L., Able, K.W., Childers, D.L., Egglestone D.B., Gillanders, B.M., Halpern, B.S., Hays, C.G., Hoshino, K., Minello, T.J., Orth, R.J., Sheridan, P.F., Weinstein, M.P., 2003. The role of nearshore ecosystems as fish and shellfish nurseries. Issues in Ecology No. 11. Ecological Society of America.

Chen, Z., Canil, D., Longerich, H.P., 2000. Automated in situ trace element analysis of silicate materials by laser ablation inductively coupled plasma mass spectrometry. Fresenius J. Anal. Chem. 368, 73–78.

Cushing, D.H., 1981. Fisheries Biology, 2nd ed. University of Wisconsin Press, Madison, WI.

Dorval, E., Jones, C.M., Hannigan, R., van Montfrans, J., 2005. Can otolith chemistry be used for identifying essential seagrass habitats for juvenile spotted seatrout, *Cynoscion nebulosus*, in Chesapeake Bay? Mar. Freshwat. Res. 56 (5).

Eastman, J.T., 1993. Antarctic Fish Biology: Evolution in a Unique Environment. Academic Press, San Diego.

Evseenko, S.A., Kock, K.-H., Nevinsky, M.M., 1995. Early life history of the Patagonian toothfish *Dissostichus eleginoides* Smitt, 1898 in the Atlantic Secot of the Southern Ocean. Antarctic Sci. 7 (3), 221–226.

Fach, B.A., Klinck, J.M., 2006. Transport of Antarctic krill (*Euphausia superba*) across the Scotia Sea. Part I: circulation and particle tracking simulations. Deep-Sea Res. I 53, 987–1010.

Glorioso, P.D., 2002. Modelling the South West Atlantic. Aquatic Conserv. Mar. Freshwat. Ecosyst. 12, 27–37.

Harden Jones, F.R., 1968. Fish Migration. Edward Arnold, London, 325 pp.

Horn, P.L., 2002. Age and growth of Patagonian toothfish (*Dissostichus eleginoides*) and Antarctic toothfish (*D. mawsoni*) in waters from the New Zealand subantarctic to the Ross Sea, Antarctica. Fish. Res. 56, 275–287.

Jones, C.M., Chen, Z., 2003. New techniques for sampling larval and juvenile fish otoliths for trace-element analysis with laser-ablation sector-field inductively-coupled plasma mass spectrometry (SF-ICP-MS). In: Browman, H.I., Skiftesvik, A.B. (Eds.), The Big Fish Bang: Proceedings of the 26th Annual Larval Fish Conference. Institute of Marine Research, Bergen, Norway, pp. 431–443.

Khattree, R., Naik, D.N., 1999. Applied Multivariate Statistics with SAS® Software, second ed. SAS Institute Inc., Cary, NC.

Kingsford, M.J., 1993. Biotic and abiotic structure in the pelagic environment: importance to small fishes. Bull. Mar. Sci. 53 (2), 393–415.

Kruskal, J.B., Wish, M., 1978. Multidimensional Scaling. Sage Publications, Beverley Hills.

Krusic-Golub, K., Green, C., Williams, R., 2005. First increment validation of Patagonian toothfish (*Dissostichus eleginoides*) from Heard Island. CCAMLR Sci. Papers no. WG-FSA-05/61.

Kuehl, R.O., 1994. Statistical Principles of Research Design and Analysis. Duxbury Press, Belmont, CA.

Laptikhovsky, V., Brickle, P., 2005. The Patagonian toothfish fishery in Falkland Islands waters. Fish. Res. 74 (1–3), 11–23.

Laptikhovsky, V., Arkhipkin, A., Brickle, P., 2006. Distribution and reproduction of the Patagonian toothfish *Dissostichus eleginoides* Smitt around the Falkland Islands. J. Fish. Biol. 68, 849–861.

Loeb, V.J., Kellermann, A.K., Koubbi, P., North, A.W., White, M.G., 1993. Antarctic larval fish assembalges: a review. Bull. Mar. Sci. 53 (2), 416–449.

Murphy, E.J., Thorpe, S.E., Watkins, J.L., Hewitt, R., 2004. Modeling the krill transport pathways in the Scotia Sea: spatial and environmental connections generating the seasonal distribution of krill. Deep-Sea Res. II 51, 1435–1456.

Naveiro-Garabato, A.C., Heywood, K.J., Stevens, D.P., 2002. Modification and pathways of Southern Ocean deep waters in the Scotia Sea. Deep-Sea Res. I 49, 681–705.

Nevinski, M.M., Kozlov, A.N., 2002. The fecundity of the Patagonian toothfish *Dissostichus eleginoides* around South Georgia Island (South Atlantic). J. Ichthyol. 42 (7), 548–550.

North, A.W., 2002. Larval and juvenile distribution and growth of Patagonian toothfish around South Georgia. Antarctic Sci. 14 (1), 25–31.

Orsi, A.H., Whitworth, T., Nowlin, W.D., 1995. On the meridional extent and fronts of the Antarctic Circumpolar Current. Deep-Sea Res. I 42 (5), 641–673.

Popper, K., 1959. The Logic of Scientific Discovery. Hutchinson, London.

Pulliam, H.R., 1988. Sources, sinks and population dynamics. Am. Naturalist 132, 652–661.

Renner, A.H.H., Heywood, K.J., Thorpe, S.E., 2009. Validation of three global ocean models in the Weddell Sea. Ocean Model., doi:10.1016/j.ocemod.2009.05.007.

Rogers, A.D., Morley, S., Fitzcharles, E., Jarvis, K., Belchier, M., 2006. Genetic structure of Patagonian toothfish (*Dissostichus eleginoides*) populations on the Patagonian Shelf and Atlantic and western Indian Ocean sectors of the Southern Ocean. Mar. Biol. 149 (4), 915–924.

Saunders, P.M., Coward, A.C., de Cuevas, B.A., 1999. Circulation of the Pacific Ocean seen in a global ocean model: Ocean Circulation and Climate Advanced Modelling project (OCCAM). J. Geophys. Res. 104 (C8), 18281–18299.

Schiffman, S.S., Reynolds, M.L., Young, F.W., 1981. Introduction to Multidimensional Scaling: Theory, Methods, and Applications. Academic Press.

Shaw, P.W., Arkhipkin, A.I., Al-Khairulla, H., 2004. Genetic structuring of Patagonian toothfish populations in the Southwest Atlantic Ocean: the effect of the Antarctic Polar Front and deep water troughs as barriers to genetic exchange. Mol. Ecol. 13 (11), 3293–3303.

Sinclair, M., 1988. Marine Populations: An Essay on Population Regulation and Speciation. University of Washington Press, Seattle, WA.

Sinclair, M., Iles, T.D., 1989. Population regulation and speciation in the oceans. J. Cons. Int. Explor. Mer. 45, 165–175.

Sprintall, J., 2003. Seasonal to interannual upper-ocean variability in the Drake Passage. J. Mar. Res. 61, 27–57.

Thorpe, S.E., Stevens, D.P., Heywood, K.J., 2005. Comparison of two time-variant forced eddy-permitting global ocean circulation models with hydrography of the Scotia Sea. Ocean Model. 9, 105–132.

Thorpe, S.E., Murphy, E.J., Watkins, J.L., 2007. Circumpolar connections between Antarctic krill (*Euphausia superba* Dana) population: investigating the roles of ocean and sea ice transport. Deep-Sea Res. I 54, 792–810.

Thorrold, S.R., Latkoczy, C., Swart, P.K., Jones, C.M., 2001. Natal homing in a marine fish metapopulation. Science 291, 297–299.

Upton, J., Shaw, C.J., 2002. An overview of the oceanography and meteorology of the Falkland Islands. Aquatic Conserv. Mar. Freshwat. Ecosyst. 12, 15–25.

Walther, B.D., Thorrold, S.R., 2006. Water, not food, contributes the majority of strontium and barium deposited in the otoliths of a marine fish. Mar. Ecol. Prog. Ser. 311, 125–130.

Ward, P., Whitehouse, M., Meredith, M., Murphy, E., Shreeve, R., Korb, R., Watkins, J., Thorpe, S., Wood-Walker, R., Brierley, A., Cunningham, N., Grant, S., Bone, D., 2002. The Southern Antarctic Circumpolar Current Front: physical and biological coupling at South Georgia. Deep-Sea Res. I 49, 2183–2202.

Webb, D.J., de Cuevas, B.A., 2003. The region of large sea surface height variability in the Southeast Pacific Ocean. J. Phys. Oceanogr. 33, 1044–1056.

Webb, D.J., de Cuevas, B.A., Coward, A.C., 1998. The First Main Run of the OCCAM Global Ocean Model. Southampton Oceanography Centre, Internal Document 34.

Williams, R., Tuck, G.N., Constable, A., Lamb, T., 2002. Movement, growth and available abundance to the fishery of *Dissostichus eleginoides* Smitt, 1898 at Heard Island derived from tagging experiments. CCAMLR Sci. 9, 33–48.